D/H analysis of minerals by ion probe

E. DELOULE, C. FRANCE-LANORD and F. ALBARÈDE

Centre de Recherches Pétrographiques et Géochimiques, et Ecole Nationale Supérieure de Géologie,
BP 20, 54501 Vandoeuvre Cedex, France

Abstract—D/H ratios with a precision of ±10 per mil have been measured by ion microprobe on 13 amphiboles, 7 biotites, and 3 muscovites of different chemical compositions previously analyzed for major elements by electron probe and for D/H ratios by standard mass spectrometry. Amphiboles have Fe/(Fe + Mg) ratios of 0.06 to 1 (actinolite, edenite, pargasite, richterite, kaersutite, arfvedsonite). The instrumental D/H fractionation factor α_{ins}, taken as D/H_{SIMS} divided by D/H_{MS}, ranges from 0.47 to 0.61. Such a variation greatly exceeds the reproducibility of the measurements on each sample and must result from a matrix effect. Calibration of the fractionation as a function of chemical composition allows the D/H ratio of hydrous minerals to be measured *in situ* by ion microprobe. A strong correlation between α_{ins} and the total electronegativity of the surrounding octahedral cations is observed for both amphiboles and micas, and indicates that fractionation depends essentially on the strength of the OH bond. The relation between D/H fractionation and ion energy is opposite to that commonly observed and invalidates the bond-breaking model for H^+ sputtering. Fitting the hydrogen energy spectrum with different distribution laws supports a model in which repeated absorption of near-infrared photons initially captured by the surrounding elements increases the OH stretching energy until a H^+ is emitted.

INTRODUCTION

THE FIRST ATTEMPTS to use the ion probe for D/H ratio measurements by HINTON *et al.* (1983) and ZINNER *et al.* (1983) were made on meteoritic samples and strastospheric dust for which isotopic variations ($\delta D = -500$ to $+4500$) could be expected to exceed greatly the large and variable instrumental fractionations reported by the authors (>100 per mil). The present work describes an analytical procedure for *in situ* measurement of hydrogen isotope compositions by ion probe applicable to terrestrial hydrous minerals, principally amphiboles but also micas. It is useful to be able to measure the δD value of individual minerals from, for example, mantle xenoliths, mixed mineral populations associated with superimposed alteration, or hydrothermal processes, or to characterize D/H zoning. As the δD values of most terrestrial samples lie in the range -200 to $+20$, a precision of ±10 per mil provides significant results. The present study is devoted primarily to the understanding of the chemical factors which determine instrumental D/H fractionations in amphiboles. Some biotites and muscovites were also analyzed in order to assess the effects of crystallographic parameters.

ANALYTICAL PROCEDURE

Crystals are mounted in epoxy, polished, gold coated, and stored in an oven at 70°C in order to minimize water adsorption. Poor reproducibility is achieved for muscovite and this is ascribed to strong crystal orientation effects. Therefore, an aliquot of the muscovite is gently powdered in an agate mortar and pressed as a flat pellet, 5 mm in diameter, before mounting as above.

A negative primary oxygen beam, with intensity ranging from 2 to 5 mA, is focused to produce a 10 μm wide beam and scanned over 25 μm. The secondary beam, permanently realigned with the principal axis by a dynamic transfer optical device, is centered in a 60 μm image field aperture. This is small enough to obtain high resolving power and wide enough to transmit the whole beam, including its spatial aberration due to the use of the widest contrast aperture. Mass resolution is set at 1300 in order to separate D^+ from H_2^+ ions. Magnet control was modified for better resolution by narrowing the field range from 300 to 50 amu. Positive secondary ions of hydrogen and deuterium are collected as single atomic ions. H, H_2, and D are measured by peak switching, the H_2 peak being included to improve the magnet settings on D. The flat peak top comprises five magnet DAC units within a few per mil of the maximum intensity (Fig. 1). As the drift of the magnetic field over an hour exceeds the peak width, the three central DAC channels are counted. Every five minutes, the position of the H peak center is updated, and the field adjustment is estimated for D and H_2 from the drift of the magnetic field on H. When counting statistics become precise enough, *i.e.* after about an hour, an intrinsic adjustment is made.

No energy filtering is applied and the energy slit is kept wide open. The electron multiplier is used in the counting mode. For H, the counting rates range from 30,000 to 100,000 cps. Counting times of 3, 2, and 15 seconds are used for H, H_2, and D, respectively, and waiting time is 1.5 seconds. Successive measurement cycles are accumulated for 90 to 120 minutes on the same sample position until good counting statistics are achieved on D (≈ 5 per mil).

Moisture from evaporation of absorbed water in the ion probe favors formation of hydrides. The D/H ratio of moisture is very low, and so the presence of moisture increases the H_2/H ratio and decreases the D/H ratio (Fig. 2). Special care is taken to remove moisture by baking the sample and ion probe at 120°C, and using a liquid nitrogen trap. When the H_2/H ratio is reduced to lower than 10^{-3}, there is no contribution of the low D/H moisture component (Fig. 3). Analyses are carried out only
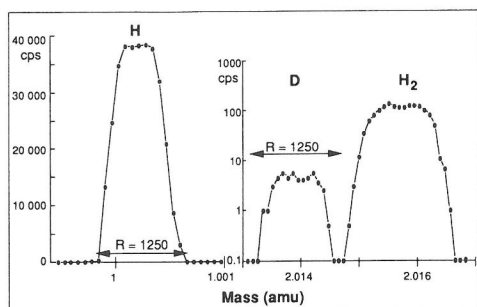
FIG. 1. High resolution mass spectrum of H, D, and H_2 ions. Primary beam intensity of 5 nA, beam size of 15 μm, image field aperture 60 μm, energy slit wide open, full magnetic field range 50 amu.

under the conditions where the H_2/H ratio is less than 8 $\times 10^{-4}$. This value is probably characteristic of H_2 production during the analysis of water-bearin minerals in a water-free environment.

The size of the sputtered area is about $30 \times 30 \ \mu$m and the hole is up to 6 μm deep. It corresponds to about 10 nanograms of amphibole and 20 picomoles of hydrogen. A conventional analysis by mass spectrometry may involve tens to hundreds of micromoles. Calculation of the useful hydrogen yield for SIMS isotopic measurement suggests a value of about 10^{-4}. The long-term reproducibility of measurements on the same mineral is better than 10 per mil (Fig. 4).

Major elements were analyzed with similar primary beam adjustments, no energy offset, and the energy slit open at ± 20 V. H, Li, F, Na, Mg, Al, Si, K, Ca, Ti, Cr, Mn, and Fe beams were measured. As O^+ and Cl^+ abundances were found to be very low, their measurement was discontinued. Mass resolution was set at a high value (4500) to overcome isobaric interferences, essentially hydrides and oxides. The Ca and Cr peaks were corrected

FIG. 3. D/H and H_2/H ratios of different amphiboles upon overnight baking of the sample and ion probe with cold trap in use.

for respective Ti and Fe contributions. For each element having at least two isotopes, possible interferences were monitored by measuring one major and one minor isotope of the same element concurrently and checking the isotopic ratios against accepted values. Oxide and hydride molecular compounds and the doubly-charged ions were found to represent less than a few per cent of their corresponding atomic singly-charged ion: for instance, a typical value of a few 10^{-4} was measured for the H_2/H ratio. Counting rates were kept under 500,000 cps and dead time was corrected. Achievement of reproducible analytical conditions was given a very high priority.

RESULTS

The standard minerals consist of single crystals, 13 amphiboles, 7 biotites, and 3 powdered muscovites, for which chemical compositions and δD were determined by electron probe and conventional mass spectrometry, respectively (Table 1). Standard amphibole minerals were selected in order to cover a broad range of Fe and Mg content, with $Fe/(Fe + Mg)$ ratios of 0.06 to 1 (actinolite, edenite,
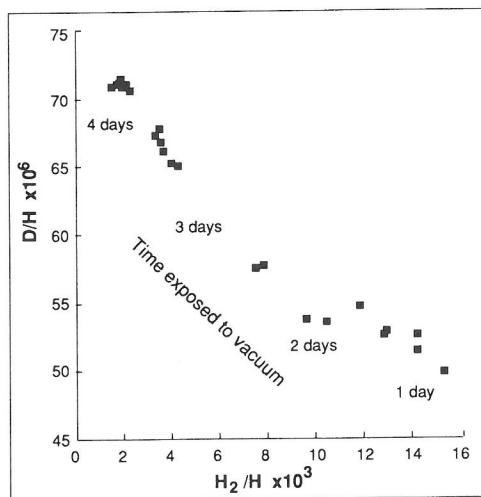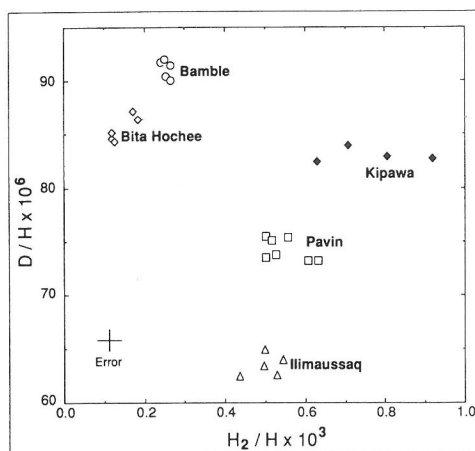

FIG. 2. Evolution of D/H and H_2/H ratios with time spent in the evacuated ion probe for the amphibole sample Etoile. Sample and ion-probe not baked, no cold trap.
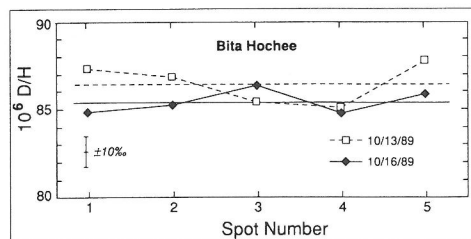

FIG. 4. Long-term reproducibility of D/H measurements. Analyzed area: $30 \times 30 \ \mu$m; measurement duration: 1.5 hours. Analyzed spots spaced by 125 μm. Horizontal lines represent the mean value for five analyses.

pargasite, richterite, kaersutite, and arfvedsonite). On each sample, the D/H ratio was measured on 10 to 20 points distributed over different minerals from the same sample. The instrumental D/H fractionation factor α_{ins} corresponds to the ratio of D/H measured by SIMS to the absolute D/H determined from measured δD values and absolute D/H ratio for SMOW (HAGEMANN et al., 1970). α_{ins} is highly variable between 0.47 to 0.61 (Table 1). Such a variation exceeds the reproducibility of the measurements on each sample and is therefore likely to result from a matrix effect.

Quite frequently, instrumental isotopic fractionation in non-metallic solids decreases linearly with the reciprocal of emission velocity v_i calculated as $(2E/M)^{1/2}$ where E and M are the ion energy and mass, respectively (SLODZIAN et al., 1980). The curve representing the measured distribution of energy or energy spectrum of hydrogen is reported in Fig. 5. Two difficulties arise in obtaining such a curve. First, since the energy slit cannot be narrowed indefinitely without a dramatic loss in sensitivity, the measured intensity represents an average over a finite energy interval. This biases somewhat the results for regions with sharp gradients. Secondly, positioning of the energy window relative to the optical of the probe and charge build-up on the sample surface make the absolute position of zero energy uncertain. However, since only ions with positive energy may be extracted from the surface, it will be assumed that the zero energy level coincides with the well-defined onset of the signal as energy increases. Noticeably, α_{ins} for amphibole is positively correlated with v_i^{-1}, with a decrease of D emissivity relative to H for increasing emission velocity (Fig. 6).

In order to assess possible relations between instrumental mass fractionation and elemental emissivity in amphiboles, beam intensities were also measured for major elements. Matrix effects on instrumental D/H fractionation were calibrated empirically as a function of the beam intensity of major chemical species and the regression coefficients calculated with a standard commercial package. Elements which did not contribute significantly to the quality of the fit (i.e. those which have no effect on the probable error) were progressively dropped out in order to make the regression as overconstrained as possible. The best fit was obtained for the following equation:

$$\alpha_{ins} = 0.56975 + 0.00604 I_{Si} - 0.00056 I_{Ca}$$
$$- 0.01799 I_{Ti} - 0.16976 I_{Mn} \quad (1)$$

where I_j refers to the beam intensity of the element j corrected for isotopic abundances and normalized to a unit sum over all measured elements. The probable error of the fit is 0.00376, which amounts to an average uncertainty of less than 7 per mil (Fig. 7). Si and Mn induce the strongest shifts of α_{ins}, while the effects of Ca and Ti are fairly small (Fig. 8). It is rather surprising to find that Mn produces a more significant shift than, for instance, Fe, which is ten times more concentrated. The reason is largely fortuitous. Fe and Mn being well-correlated and both measured accurately, the present procedure which selects only independent parameters produces more precise results with only one of them; for the present set of samples, this happens to be Mn.

Understanding the empirical relation (1) requires the assessment of hydrogen emissivity with respect to the emissivity of other elements. The elemental ionization yields relative to Si (RIY) for an element j is calculated from

$$RIY_j = \frac{I_j/C_j}{I_{Si}/C_{Si}} \quad (2)$$

where C refers to the concentration of the elements j and Si measured by electron probe. Average RIY_j values vary from 0.06 for H to ca. 44 for K. For all measured elements the RIY_j value varies by an order of magnitude among the different amphiboles (Table 2). From previous studies (ANDERSEN and HINTHORNE, 1973), it is known that RIY_j is inversely correlated with the first ionization potential (Fig. 9). As for α_{ins}, RIY_j values were handled as a linear combination of the beam intensity of the major elements and the significant coefficients calculated by linear regression. A good fit is obtained for each element, implying that amphibole composition can be calculated from measured secondary beam intensities.

It has been shown by SHIMIZU (1986) that ion emissivity in silicates increases with Si content. In amphiboles this is true only for Na, K, and Ca which have a large ionic radius. For other elements, the RIY_j values decrease when the silica content increases. Cross-effects of elements other than Si are complex; in general, Ca enhances, and Mg and Mn decrease the emissivity of most elements except H. H seems to be controlled by a markedly different sputtering mechanism, its very low emissivity being enhanced by Al and depressed by Ca and Ti. Metal hydride formation could selectively depress H^+ emissivity. Therefore, the beam intensity has been measured for the hydride species of all the major elements, both in positive and negative secondary ions. The H distributions among H-bearing species are reported in Fig. 10. Metal hydride intensities are always less than 1% relative to the metal inten-

Table 1. Structural formula, δD values and D/H instrumental

Sample	Type	Si	Al_{tetr}	Al_{oct}	Fe^{II}	Fe^{III}	Mg	Mn
Amphibole								
PavinA	Mg Kaers.	5.64	2.36	0.14	1.17	0.12	2.94	0.01
MtEmma	Pargasite	6.01	1.95	0.47	0.88	0.33	3.14	0.01
Kipawa	Mg Hast.	6.75	1.25	0.22	1.33	0.27	3.13	0.03
LacKip	Richterite	8.00	0.01	0.08	1.08	0.00	3.75	0.05
BitaHochee	Mg Kaers.	6.07	1.93	0.23	1.28	0.12	2.90	0.01
Bamble	Mg Hast.	7.38	0.62	0.12	0.84	0.17	3.87	0.01
PavinB	Mg Kaers	5.79	2.21	0.23	1.23	0.02	2.88	0.01
IlimaussaqB	Fe Richt.	7.98	0.02	0.34	4.26	0.00	0.09	0.05
AlpesFA	Pargasite	5.87	2.13	0.71	0.95	0.43	2.85	0.02
Australia DV	Richerite	7.66	0.07	0.00	0.29	0.00	4.63	0.01
Mickland	Mg Hast.	7.53	0.45	0.14	0.81	0.14	3.92	0.01
AlpesUR	Gedrite	7.57	0.43	0.26	0.71	0.17	3.89	0.04
Seljas	Tremolite	7.99	0.01	0.00	0.92	0.00	4.21	0.01
Etoile	Mg Kaers.	5.84	2.13	0.38	1.00	0.18	2.95	0.01
IlimaussaqA	Mg Arfv.	8.13	0.00	0.16	3.85	0.58	0.00	0.09
Biotite								
BE 114		5.42	2.58	0.60	1.45	0.30	3.26	0.01
M 114		5.46	2.54	0.75	1.74	0.30	2.75	0.01
NA 28		5.45	2.55	0.89	2.30	0.07	2.21	0.01
D 14		5.45	2.55	0.98	3.05	0.00	1.18	0.02
D 65		5.48	2.52	1.08	2.39	0.42	0.96	0.04
U 315		5.42	2.58	1.12	2.86	0.42	0.64	0.09
X 77		5.46	2.54	1.44	2.48	0.44	0.55	0.09
Muscovite								
D 14		6.16	1.84	3.62	0.27	—	0.16	0.00
DK 127		6.25	1.75	3.65	0.34	—	0.09	0.01
NL 506		6.16	1.84	3.66	0.26	—	0.14	0.00

Chemical compositions measured by electron microprobe except for Li measured by atomic absorbtion and H_2 measured manometrically after quantitative extraction. Structural formulas of amphibole are calculated according to PAPIKE *et al.* (1974). m/c: mean mass/charge ratio for the octahedrally coordinated cations (SUZUOKI and EPSTEIN, 1976). TEN: total electronegativity of the M(1,3) site. δD measured by mass spectrometry (*e.g.* FRANCE-LANORD *et al.* 1988). α_{ins}: instrumental fractionation as $(D/H_{IMS})/(D/H_{MS})$. Data for micas are from FRANCE-LANORD (1987) and FRANCE-LANORD *et al.* (1988) and for IlimaussaqB amphibole from SHEPPARD (1986).

sities. In the positive secondary beam, H^+ is largely dominant, the main hydrides (Mg, Ca, Si, Al, in this order) being less than ten per cent of the total. Conversely, the dominant negative secondary species are OH^- and H^-, with an OH^-/H^- ratio of about five. Due to the very low emissivity of the metals as negative ions, the negative hydrides (CaH^-, MgH^-, SiH^-) are less abundant than their positive counterparts.

DISCUSSION

Instrumental fractionation

Most published data on isotopic effects in ionization process concern pure metals (*e.g.* SHIMIZU and HART, 1982a,b; SOEDERVALL *et al.,* 1988) or simple salts and oxides (*e.g.* SLODZIAN *et al.,* 1980; LORIN *et al.,* 1982; CHAUSSIDON and DEMANGE, 1988; GNASER and HUTCHEON, 1988). As hydrogen is a minor element, even in hydrous minerals, hydrogen-hydrogen effects are expected to be insig-

nificant compared to those of hydrogen-silicate. The lighter isotopes are preferentially extracted, and this effect is more pronounced for light elements because of their larger relative mass difference. Mass fractionation has been suggested to depend on (i) the mass ratio of the isotopes, (ii) the strength of the chemical bond between the analyzed ion and its matrix, (iii) the work function of the surface, and (iv) the energy of the secondary ions. Due to the large relative mass difference between D and H, a large mass fractionation in sputtering and ionization was anticipated.

The bond breaking model (SLODZIAN *et al.,* 1980), widely accepted for ionic solids, predicts that fractionation depends on ion emission velocity. The isotopic fractionation α_{ins} is the relative difference of the ionization probability of isotope i and j, and can be expressed as

$$F_{ji} = \alpha_{ins} - 1 = \frac{P_j}{P_i} - 1 \# - \frac{M_0 v_0}{v_i} \qquad (3)$$

fractionation of the standard amphiboles and biotites.

Ti	Cr	Ca	Na	K	Li	F	Cl	OH	m/c	TEN	δD	α_{ins}
0.66	0.001	1.92	0.66	0.23	—	0.067	0.022	0.98	15.82	4.051	−48	0.543
0.32	0.011	1.70	0.73	0.29	—	0.032	0.011	1.40	14.81	4.019	−50	0.576
0.09	0.006	1.75	0.72	0.20	0.029	0.344	0.151	1.45	16.41	4.051	−88	0.563
0.02	0.001	0.84	1.85	0.43	—	1.310	0.002	0.57	15.68	3.878	−112	0.573
0.49	0.002	1.73	0.71	0.37	—	0.023	0.016	1.27	16.11	4.051	−52	0.542
0.04	0.002	1.83	0.45	0.05	0.002	0.043	0.031	1.99	14.83	3.794	−61	0.591
0.64	0.001	1.91	0.63	0.23	—	0.038	0.015	0.97	15.89	4.050	−48	0.543
0.08	0.000	0.38	2.96	0.18	—	0.152	0.004	1.05	26.04	4.861	−190	0.480
0.04	0.000	1.99	0.84	0.08	0.005	0.004	0.004	4.17	15.32	3.911	−100	0.556
0.34	0.000	1.03	0.91	0.99	—	1.505	0.003	0.21	12.22	3.730	−149	0.597
0.04	0.002	1.82	0.38	0.04	0.001	0.022	0.014	1.98	14.72	3.900	−60	
0.01	0.054	1.73	0.19	0.01	0.005	0.008	0.006	2.34	14.21	3.843	−52	0.591
0.00	0.001	1.85	0.03	0.00	—	0.004	0.010	2.09	14.64	3.784	−64	0.607
0.56	0.002	1.67	0.77	0.28	0.001	0.019	0.017	0.83	15.18	4.054	−112	0.568
0.07	0.000	0.06	2.32	0.68	0.606	0.085	0.003	2.38	25.91	4.945	−142	0.469
0.19	—	0.00	0.20	1.50	—	—	—	2	16.11	4.163	−68	0.566
0.20	—	0.00	0.03	1.57	—	—	—	2	16.87	4.263	−87	0.546
0.23	—	0.00	0.16	1.57	—	—	—	2	18.11	4.356	−81	0.517
0.31	—	0.00	0.04	1.83	—	—	—	2	20.32	4.765	−188	0.493
0.25	—	0.00	0.00	1.68	0.550	—	—	2	18.25	4.470	−99	0.504
0.21	—	0.00	0.05	1.88	—	—	—	2	20.69	4.711	−162	0.507
0.24	—	0.00	0.03	1.68	—	—	—	2	19.54	4.703	−99	0.513
0.05	—	0.00	0.14	1.80	—	0.003	0.000	2	9.86	2.996	−184	0.636
0.01	—	0.00	0.12	1.79	—	0.235	0.000	2	10.63	3.012	−84	0.637
0.02	—	0.00	0.57	1.39	—	0.045	0.000	2	10.33	3.000	−57	0.644

where P_i is the ionization probability of atom i, v_i its emission velocity, v_0 a constant for a given matrix, and $M_0 = (M_j/M_i)^{1/2} - 1$, M_j and M_i being the atomic mass. This relation has received further support from later studies of SLODZIAN (1982), SROUBEK (1988), GNASER and HUTCHEON (1988), GOLDBERG et al., (1988), and SOEDERVALL et al., (1988). Although the average RIY_j of each element is indeed roughly inversely related to the first ionization potential (Fig. 9), which is an essential feature of this model (YU, 1988), the dependence of D/H fractionation in amphibole with emission velocity is opposite to what the bond breaking model predicts (Fig. 6). A low yield for hydrogen relative to those of most other cations could be taken as supporting a model of self-ionization of excited atoms (YU, 1988), which is known to describe adequately light atom sputtering (SROUBEK, 1988). However, the equation proposed by YU (1988) for transition probability predicts that isotopic fractionation is independent of emission velocity, which makes this model unacceptable.

Few other cases of inverse relationships between mass fractionation and emission velocity have been observed; they seem to be restricted to metals (SHIMIZU and HART, 1982a,b). Interatomic forces in metals, however, cannot be compared to those in silicates.

Even though conventional models fail to predict the positive correlation of fractionation with v^{-1}, several arguments support control of the hydrogen yield by its bonding energy with the surrounding atoms. SUZUOKI and EPSTEIN (1976) showed that, at a given temperature, D/H fractionation between OH-bearing minerals and water is strongly correlated with the mean atomic mass/charge (m/c) ratio of the octahedrally coordinated cations. α_{ins} values are reported in Fig. 11 for amphiboles, biotites, and muscovites against the m/c ratio. The linear array calculated for these three minerals has a probable error of 0.011. Although this empirical correlation is difficult to account for quantitatively in terms of a simple physical model, consistent variations for
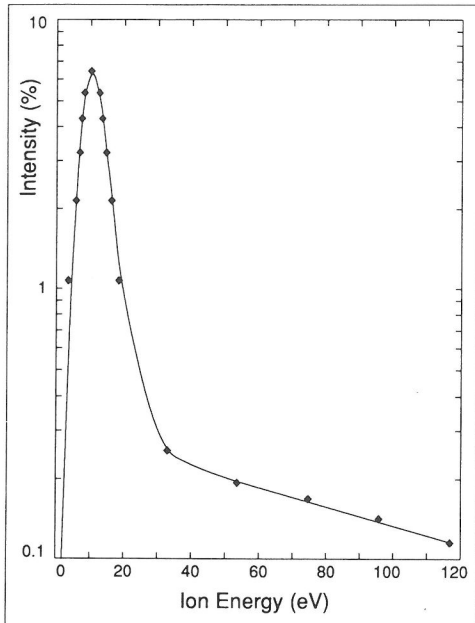
FIG. 5. Full diamonds: measured energy spectrum of hydrogen ions with energy slit open at ± 2.5 V. Charge buildup makes absolute energy offset uncertain by ± 2 V. The curve represents the energy distribution fitted through Eqns. (6) and (7).

FIG. 6. D/H instrumental fractionation (α_{ins}) vs. emission velocity ($1/v$) for hydrogen sputtered from the amphibole sample Lac Kip. The energy slit width is open at ± 5 V.

widely different structures supports control of D/H fractionation by the configuration and/or bonding energy of the OH-sites.

The good correlation of α_{ins} with the product of the mean electronegativity (MEN) by the number $N_\diamond$ of octahedral cations surrounding OH shown in Fig. 12 allows a better formulation involving the energy of the oxygen-hydrogen bond. HAWTHORNE (1981) reviewed the infrared data relevant to the variation of the O-H bond strength in amphibole with the nature of surrounding octahedral cations, the fundamental O-H stretching band shifting from 3675 cm^{-1} for a magnesian-cummingtonite end member to 3615 cm^{-1} for a ferro-actinolite end member. In addition, MEN is also known to be extremely well correlated with the frequency shift of the infrared absorption lines, and therefore with the O-H bond energy. The same dependence of the O-H bond shift on the nature of the octahedral cations and its correlation with their MEN are observed for micas (VELDE, 1983; ROSSMAN, 1984). The frequency shifts are 96 cm^{-1} per MEN unit in trioctahedral micas, 170 cm^{-1} for dioctahedral micas (VELDE, 1983), and 100 cm^{-1} for amphiboles (HAWTHORNE, 1981). Amphibole data suggest that the shift of the OH bond strength due to each octahedral cation is reasonably additive. Hence, a convenient measure of the relative bond strength
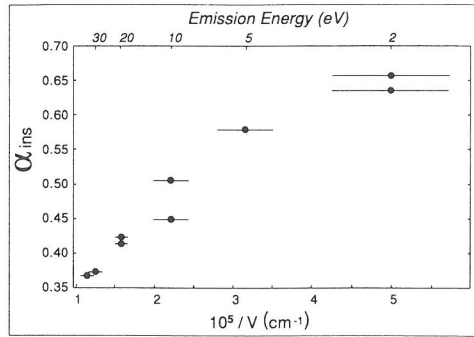
will be the sum of the contribution of each neighbor which we take as the product of $N_\diamond$ by MEN, with $N_\diamond$ set to two for muscovite and three for biotite and amphibole. Figure 12 is a strong indication that for the three different hydrous minerals, the structural environment, which ultimately controls the strength of the O-H bond, is the predominant control of the D/H fractionation.

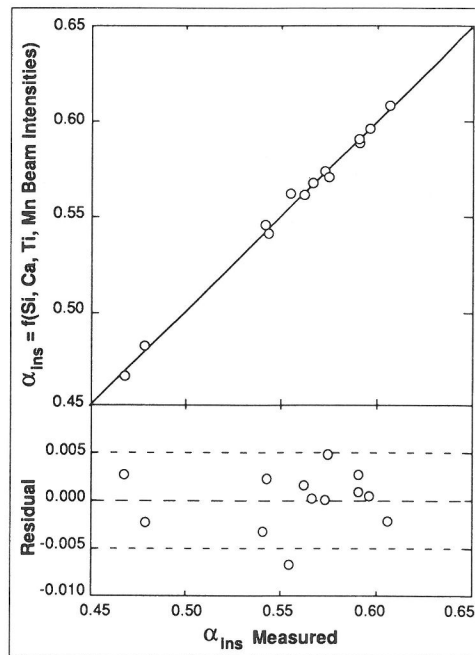Nevertheless, it is known that non-octahedral cations also affect O-H stretching. Na and K in the

FIG. 7. Comparison of the values calculated from Si, Ca, Ti, and Mn beam intensities through Eqn. (1) (top) and residual errors (bottom) with the measured α_{ins} values.
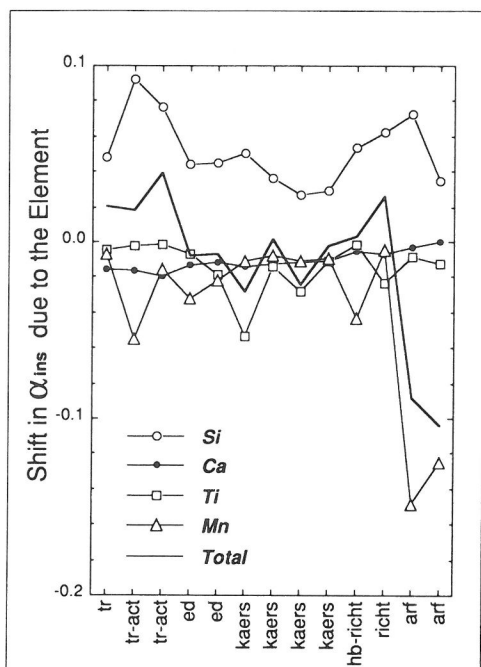
FIG. 8. Contribution of Si, Ca, Ti, and Mn beam intensities to the variation of the D/H instrumental fractionation factor α_{ins}, as calculated from Eqn. (1), on each of the standard amphiboles.

FIG. 9. Mean values of element ionization yield relative to Si (RIY_j) as a function of the first ionization energy for the major element measured in amphiboles.

ing frequency by about 2 cm^{-1} (HAWTHORNE, 1981). Because of these complex effects, the relation displayed in Fig. 12 is no more than a good first-order physical model valid for different hydrous phases. For practical purposes, an empirical calibration of the D/H fractionation with amphibole composition can be expected to provide better results.

As hydrogen isotope fractionation is related to mineral structure, most of the hydrogen ionization should occur below the layer disturbed by the sputtering process (= mixing layer) without later recombination. Unfortunately, the thickness of this mixing layer, which is known to be some 10 nm in the case of semi-conductors and metals at 10 kV (HOFMANN, 1982; ARMOUR et al., 1988), is unknown for silicates.

"A" sites of amphiboles raises the frequency by about 60 cm^{-1} in the richterite-tremolite series (ROWBOTHAM and FARMER, 1973), by 30–40 cm^{-1} for hastingsite and pargasite (SEMET, 1973), by 24 cm^{-1} in riebeckite (STRENS, 1974), and GRAHAM et al. (1984) suggested that these cations could affect D-H fractionation between water and amphiboles. Ca in the M(4) positions also increases the stretch-
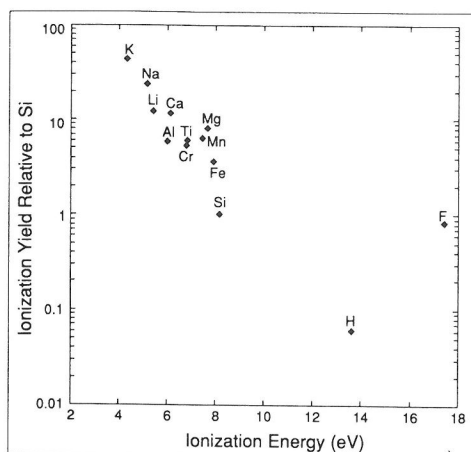
Table 2. Ionization yield relative to Si for standard amphiboles.

|	H/Si	F/Si	Na/Si	Mg/Si	Al/Si	K/Si	Ca/Si	Ti/Si	Cr/Si	Mn/Si	Fe/Si	^{28}Si cps
PavinA	0.016	0.10	13.01	5.51	4.58	14.59	8.88	3.07	5.09	3.79	2.9	27000
MtEmma	0.026	0.40	24.40	7.84	6.43	33.09	13.06	2.53	5.44	6.76	3.25	34500
Kipawa	0.012	0.37	24.76	7.39	6.33	33.57	12.52	4.07	5.01	5.80	3.71	200660
LacKip	0.031	0.15	17.61	6.09	4.75	28.29	10.20	4.72	1.33	4.88	3.08	107000
BitaHochee	0.066	1.68	37.93	10.32	7.95	50.89	16.58	4.42	9.16	8.12	4.87	31890
Bamble	0.033	0.68	32.19	8.51	6.28	47.40	14.62	5.71	13.48	4.94	4.27	43370
PavinB	0.087	1.57	50.25	12.12	9.22	73.55	19.91	4.86	8.19	9.39	5.56	38575
IlimaussaqB	0.115	0.52	29.32	15.49	10.63	104.5	8.74	3.97	—	11.46	4.69	44720
AlpesFA	—	—	19.54	6.82	3.14	82.71	8.14	20.37	—	4.70	2.78	92290
AustrDV	0.051	0.12	13.64	5.47	4.30	17.98	8.98	2.89	—	3.68	2.77	159050
Mickland	0.010	0.35	12.71	5.14	4.29	16.91	8.51	4.58	7.73	3.21	2.68	185500
AlpesUR	0.009	0.47	9.21	5.26	2.91	15.67	8.59	7.21	0.95	4.01	2.65	243500
Seljas	0.110	2.79	—	6.89	3.69	—	11.36	—	0.92	4.25	3.14	61460
Etoile	0.205	1.99	34.86	9.44	7.47	45.77	14.60	1.29	1.62	7.33	4.07	46500
IlimaussaqA	0.086	0.33	33.45	18.13	5.14	47.38	10.59	14.08	—	11.87	3.19	39300
Average	0.061	0.823	23.33	8.69	5.81	43.738	11.72	5.985	5.36	6.28	3.58	
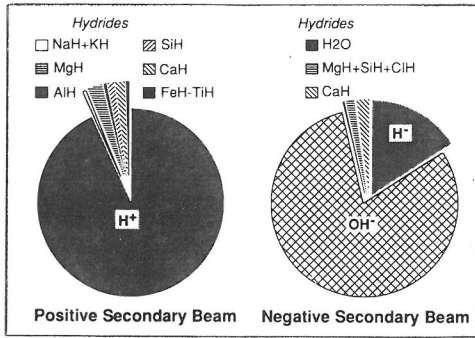
FIG. 10. Hydrogen allotment to atomic H, hydrides, and hydroxide in the secondary positive and negative ion beams. Same measurements conditions as for isotopic analyses, except for a mass resolution of 4500.

Hydrogen energy distribution

Understanding the mechanisms of hydrogen emission hinges around a discussion of the energy spectrum (Fig. 5). It can be shown that commonly accepted theoretical distributions of energy are inappropriate. Let us call $f^H(E)$ the fraction of ions with secondary energy E in the range E to $E + dE$. To a constant of normalization, $f^H(E)$ is equal to the counts per second measured at E provided the energy window is small (5 volts). The linear collision cascade of GRIES and RUEDENAUER (1975) predicts a dependence of $f^H(E)$ with E given by

$$f^H(E) \propto \frac{E}{(E + U_s)^3} \qquad (4)$$

where U_s is the surface binding energy. This equation implies a linear relation between $\dfrac{E}{f^H(E)}$ and $(E + U_s)^{1/3}$, which is not observed. The bond breaking model of SLODZIAN et al. (1980) would predict a different relation:

$$f^H(E) \propto \exp\left(-\frac{k}{\sqrt{E}}\right) \qquad (5)$$

which can be tested by searching linear arrays in a plot $\text{Log}^2 [f^H(E)]$ vs. $1/E$, but is again not observed.

Inspection of the curve (Fig. 5) suggests that it is made up of two distinct sections, a sharp peak, $f_1^H(E)$, centered at ≈ 12 eV and a gently decreasing segment, $f_2^H(E)$, above 40 eV, hinting at the superposition of distinct physical processes such as $f^H(E)$ is the sum of $f_1^H(E)$ and $f_2^H(E)$. The $f_2^H(E)$ vs. E relation at high energy is nearly perfectly exponential and can be fitted by

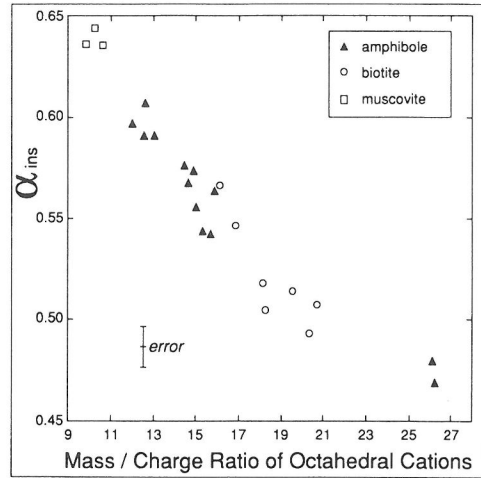$$f_2^H(E) = 3.2 \ 10^{-3} \exp(-0.0089 \pm 6E). \qquad (6)$$

FIG. 11. D/H isotopic fractionation α_{ins} vs. the mean mass to charge ratio of the octahedral cations (m/c) for amphibole, biotite, and muscovite.

Once this exponential contribution is removed from the energy spectrum, the remainder $f_1^H(E)$ was fitted with different acceptable functions such as exponential, polynomial, or power laws, but the outcome was uniformly poor. In contrast, excellent results were obtained for a fit by a gamma distribution:

$$f_1^H(E) = 2.0 \ 10^{-5} E^{7.2 \pm 3} \exp(-0.86 \pm 3E). \qquad (7)$$

The first constants in $f_1^H(E)$ and $f_2^H(E)$ have been normalized in such a way that their sum is normalized over $[0, +\infty]$.
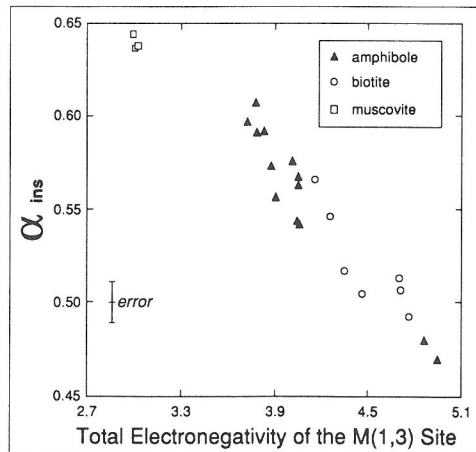
Deuterium is not abundant enough for its energy

FIG. 12. D/H isotopic fractionation α_{ins} vs. the total electronegativity ($N_\diamond \times$ MEN, see text) of ions in the M(1,3) octahedral site for amphibole, biotite, and muscovite.

spectrum to be measured accurately. However, the D/H fractionation measured at different values of E (Fig. 6) can be fitted to a power law:

$$\alpha_{ins} = c^t E^{-0.203}. \qquad (8)$$

No data are available at high energy; hence, the energy spectrum will be modelled as a simple low energy peak. Applying Eqn. (8) to the H energy spectrum in the low energy range gives upon normalization

$$f^D(E) = 2.5 \ 10^{-5} E^{6.1\pm3} \exp(-0.76 \pm 4E). \ (9)$$

The exponential form of the high energy distribution of Eqn. (6) is suggestive of a Boltzman-type energy distribution. The constant in the exponential term is $0.0089^{-1} = 112$ eV and is high enough to correspond to energy transferred during electronic excitation in the collision cascade (inelastic collision).

As far as the lower energy peak is concerned, it is well known that gamma functions such as those of Eqns. (7) and (9) are simply related to exponential distributions (*e.g.* LLOYD, 1980, p. 202): let E be a random variable distributed exponentially as $\lambda \exp(-\lambda E)$ with λ^{-1} representing the expected value of E, then the sum of m variables with the same λ value is distributed as a gamma density function:

$$f(E) = \frac{\lambda^n}{\Gamma(n)} E^{n-1} \exp(-\lambda E). \qquad (10)$$

As suggested by the relation between the yield and the bond energy, it is likely that this process has an activation threshold. The fairly good fit of the peak shape in the energy spectrum with gamma distributions suggests an additive process of energy transfer leading to ion emission. From Eqns. (7) and (9), n_H and n_D are, respectively, 8.16 and 7.10. Hence, for hydrogen, one could conceive ion emission after ≈ 8 transfers of energy "quantum" λ^{-1} of 1.16 eV above the energy required for bond rupture, whereas ≈ 7 transfers of 1.32 eV would be necessary for deuterium. This is indeed consistent with bond energies usually being stronger for deuterium than for hydrogen (HERZBERG, 1970; KERR and TROTMAN-DICKENSON, 1977). Interestingly, the average energy of emitted ions, given by $n\lambda^{-1}$, is nearly identical for hydrogen and deuterium (9.5 and 9.4 eV, respectively). The energy "quanta" λ^{-1} corresponds to wavenumbers of 9,300–10,700 cm^{-1} (near-infrared), values which fall in a range typical of photon absorption by transition elements (Fe^{2+}, Fe^{3+}, Mn^{2+}, Cr^{3+}, $\cdots$) in a distorted octahedral site (*e.g.* HAWTHORNE, 1981). OH-bond energy would therefore increase up to ion ejection as the surrounding transition element atoms absorbs the electromagnetic radiation known (BENNINGHOVEN *et al.*, 1987, p. 180) to be produced by ion bombardment.

CONCLUSIONS

The instrumental D/H fractionation during SIMS analysis is strongly correlated with the octahedrally coordinated cation for amphiboles and micas. Relations between α_{ins} and m/c ratio or MEN support its control by the H bond energy with the surrounding atoms. Using an empirical calibration of the D/H fractionation with amphibole composition, δD can be measured on a mineral smaller than 50 μm with a precision of ± 10 per mil.

Notwithstanding the relation between D/H fractionation and H bond energy, its variation with emission velocity is opposite to that which is predicted by the bond breaking model. Examination of the H and D energy spectra suggests that most H$^+$ is emitted upon repeated absorption of near-infrared photons.

REFERENCES

ANDERSEN C. A. and HINTHORNE J. R. (1973) Thermodynamic approach to the quantitative interpretation of sputtered ion mass spectra. *Anal. Chem.* **45**, 1421–1438.

ARMOUR D. G., WADSWORTH M., BADHEKA R., VAN DEN BERG J., BLACKMORE G., COURTNEY S., WHITEHOUSE C. R., CLARK E. A., SYKES D. E. and COLLINS R. (1988) Fundamental processes which affect the depth resolution obtainable in sputter depth profiling. In *SIMS VI Proceedings* (eds. A. BENNINGHOVEN, A. M. HUBER and H. M. WERNER), pp. 399–408. Wiley.

BENNINGHOVEN A., RÜDENAUER F. G. and WERNER H. W. (1987) *Secondary Ion Mass Spectrometry, Basic Concepts, Instrumental Aspects, Applications and Trends.* Wiley.

CHAUSSIDON M. and DEMANGE J.-C. (1988) Instrumental mass fractionation in ion microprobe studies of sulphur isotopic ratios. In *SIMS VI Proceedings* (eds. A. BENNINGHOVEN, A. M. HUBER and H. M. WERNER), pp. 937–940. Wiley.

FRANCE-LANORD C. (1987) Chevauchement, métamorphisme et magmatisme en Himalaya du Népal central. Etude isotopique H, C, O. Thesis, INPL, Nancy, France.

FRANCE-LANORD C., SHEPPARD S. M. F. and LE FORT P. (1988) Hydrogen and oxygen isotope variations in the High Himalaya peraluminous Manaslu leucogranite: evidence for heterogeneous sedimentary source. *Geochim. Cosmochim. Acta* **52**, 513–526.

GNASER H. and HUTCHEON I. D. (1988) The velocity dependence of isotope effects in secondary ion emission. In *SIMS VI Proceedings* (eds. A. BENNINGHOVEN, A. M. HUBER and H. M. WERNER), pp. 29–32. Wiley.

GOLDBERG E. C., FERRON J. and PASSEGGI M. C. G. (1988) Effects of the ion velocity changes on the ionization probability in secondary ion emission. In *SIMS VI Proceedings* (eds. A. BENNINGHOVEN, A. M. HUBER and H. M. WERNER), pp. 75–78. Wiley.

GRAHAM C. M., HARMON R. S. and SHEPPARD S. M. F. (1984) Experimental hydrogen isotope studies: hydrogen isotope exchange between amphibole and water. *Amer. Mineral.* **69**, 128–138.

GRIES N. H. and RUEDENAUER F. G. (1975) A quantitative model for the interpretation of secondary ion mass spectra of dilute alloys. *Intl. J. Mass Spectrum. Ion Phys.* **18**, 111–127.

HAGEMANN R., NIEF G. and ROTH E. (1970) Absolute isotopic scale for deuterium analysis of natural waters. Absolute D/H ratio for SMOW. *Tellus* **22**, 712–715.

HAWTHORNE F. C. (1981) Amphibole spectroscopy, vibrational spectroscopy, the hydroxyl stretching region. In *Amphiboles and Other Hydrous Pyriboles—Mineralogy* (ed. D. R. VEBLEN); *Reviews in Mineralogy 9a,* pp. 103–140. Mineralogical Society of America.

HAWTHORNE F. C. (1983) Quantitative characterization of site-occupancies in minerals. *Amer. Mineral.* **68**, 287–306.

HERZBERG G. (1970) The dissociation energy of the hydrogen molecule. *J. Mol. Spectrosc.* **33**, 147–168.

HINTON R. W., LONG J. V. P., FALLICK A. E. and PILLINGER C. T. (1983) Ion probe measurements of D/H ratios in meteorites. *Lunar Planet. Sci.* **XIV**, 313–314.

HOFMANN S. (1982) Disturbing effects in sputter profiling. In *SIMS III Proceedings* (eds. A. BENNINGHOVEN *et al.*), pp. 186–200. Springer.

KERR J. A. and TROTMAN-DICKENSON A. F. (1977) Strengths of chemical bonds. In *Handbook of Chemistry and Physics* (ed. R. C. WEAST), pp. F219–F229. CRC Press.

LLOYD E. (1980) Handbook of Applicable Mathematics, Vol. II: Probability (ed. W. Lederman). Wiley London, 450 p.

LORIN J. C., HAVETTE A. and SLODZIAN G. (1982) Isotope effects in secondary ion emission. In *SIMS III Proceedings* (eds. A. BENNINGHOVEN *et al.*), pp. 140–150. Springer.

PAPIKE J. J., CAMERON K. L. and BALDWIN K. (1974) Amphiboles and pyroxenes: characterization of other than quadrilateral components and estimates of ferric iron from microprobe data (abstr.). *Geol. Soc. Amer. Abstr. Prog.* **6**, 1053–1054.

ROSSMAN G. R. (1984) Spectroscopy of micas, infrared spectra. In *Micas* (ed. S. W. BAILEY); *Reviews in Mineralogy 13,* pp. 145–177. Mineralogical Society of America.

ROWBOTHAM G. and FARMER V. C. (1973) The effect of "A" site occupancy upon hydroxyl stretching frequency in clinoamphiboles. *Contr. Mineral. Petrol.* **38**, 147–149.

SEMET M. P. (1973) A crystal-chemical study of synthetic magnesiohastingsite. *Amer. Mineral.* **58**, 480–494.

SHEPPARD S. M. F. (1986) Igneous rocks: III. Isotopic case studies of magmatism in Africa, Eurasia, and oceanic islands. In *Stable Isotopes in High Temperature Geological Processes* (eds. J. W. VALLEY, H. P. TAYLOR and J. R. O'NEIL); *Reviews in Mineralogy 16,* pp. 319–372. Mineralogical Society of America.

SHIMIZU N. (1986) Silicon-induced enhancement in secondary ion emission from silicates. *Intl. J. Mass. Spectrom. Ion Proc.* **69**, 325–338.

SHIMIZU N. and HART S. R. (1982a) Isotope fractionation in secondary ion mass spectrometry. *J. Appl. Phys.* **53**, 1303–1311.

SHIMIZU N. and HART S. R. (1982b) Applications of the ion microprobe to geochemistry and cosmochemistry. *Ann. Rev. Earth Planet. Sci.* **10**, 483–526.

SLODZIAN G. (1982) Dependence of ionisation yields upon elemental composition; isotopic variations. In *SIMS III Proceedings* (ed. A. BENNINGHOVEN *et al.*), pp. 115–123. Springer.

SLODZIAN G., LORIN J. C. and HAVETTE A. (1980) Isotopic effect on the ionization probabilities in secondary ion emission. *J. Phys.* **23**, 555–558.

SOEDERVALL U., ENGSTROEM E. U., ODELIUS H. and LODDING A. (1988) Isotope mass effects in secondary ion emission. In *SIMS VI Proceedings* (eds. A. BENNINGHOVEN, A. M. HUBER and H. M. WERNER), pp. 83–88. Wiley.

SROUBEK Z. (1988) Formation of secondary ions. In: *SIMS VI Proceedings* (eds. A. BENNINGHOVEN, A. M. HUBER and H. M. WERNER), pp. 25–28. Wiley.

STRENS R. G. J. (1974) The common chain, ribbon, and ring silicates. In *The Infrared Spectra of Minerals,* pp. 305–330. Mineralogical Society, London.

SUZUOKI T. and EPSTEIN S. (1976) Hydrogen isotope fractionation between OH-bearing minerals and water. *Geochim. Cosmochim. Acta* **40**, 1229–1240.

VELDE B. (1983) Infrared OH-stretch bands in potassic micas, talcs and saponites; influence of electronic configuration and site of charge compensation. *Amer. Mineral.* **68**, 1169–1173.

YU M. L. (1988) A bond-breaking model for the sputtering of secondary ions and excited atoms. In *SIMS VI Proceedings* (eds. A. BENNINGHOVEN, A. M. HUBER and H. M. WERNER), pp. 83–88. Wiley.

ZINNER E., MCKEEGAN R. M. and WALKER R. M. (1983) Laboratory measurements of D/H ratios in interplanetary dust. *Nature* **305**, 119–121.